Transactions of the Korean Nuclear Society Autumn Meeting
Changwon, Korea, October 30-31, 2025

Temperature-Dependent Corrosion of C276, SS316 and Alloy 600 in NaCl-$MgCl_2$ Molten Salt

Seok Min Yoon[a,b], Chang Hwa Lee[b], Eun-Young Choi[a,b], Seol Kim[a,b], and Taeho Kim[a,b*]
[a]University Science and Technology (UST)
217 Gajeong-ro, Yuseong-gu, Daejeon 34113, Republic of Korea
[b]Advanced Fuel Cycle Technology Development Division, Korea Atomic Energy Research Institute (KAERI)
111 Daedeok-daero 989 beon-gil, Yuseong-gu, Daejeon 34057, Republic of Korea
[*]Corresponding author : Taeho Kim. tkim@kaeri.re.kr

1. Introduction

Molten Salt Reactors (MSRs) use molten halide salts as the primary coolant-and in some concepts as the fuel solvent-whose wide liquid range, low vapor pressure, and favorable thermophysical properties enable efficient power cycles and high-temperature applications. Among halides, chloride salts such as NaCl-$MgCl_2$ are attractive for their thermal stability and practical availability; however, their strong reactivity with metals/alloys at high temperature makes corrosion a key constraint on component life, safety margins, and design limits. In chloride environments, accelerated formation/dissolution and volatility of metal chlorides can drive selective leaching (dealloying) and subsurface penetration, leading to microstructural degradation along grain boundaries and within the matrix. In this context, direct quantitative-qualitative comparisons under the same salt chemistry are essential for materials selection and system reliability[1,2].

In this study, C276, SS316, and Alloy 600 are selected for comparison. SS316, an austenitic steel widely used in actual plant hardware, provides a baseline for 316-based structures; Alloy 600, a representative Ni-Cr-Fe alloy, serves as a reference point for assessing relative corrosion resistance within the Ni-based alloy; and C276, a Ni-Cr-Mo high-Mo alloy, is used to probe the effect of Mo addition and the behavior of more corrosion-resistant compositions. Because the principal alloying contents differ across these alloys, they are expected to respond differently in chlorides with respect to corrosion-product stability, dissolution/re-precipitation tendencies, elemental diffusion behavior, and the continuity/density of surface layers.

Temperature governs the thermal activation of metal-salt reactions, the diffusion of alloying and halogen species, the solubility/volatility of metal chlorides, and mass transport in the melt. While higher temperature generally accelerates reaction and diffusion and can intensify damage, changes in phase or precipitate stability and differences in volatilization/recondensation behavior can also shift corrosion modes. Accordingly, under the same NaCl-$MgCl_2$ chemistry we compare 650 and 550 ℃ to extract temperature-induced transitions in damage modes, alloy-specific temperature sensitivity, and the contribution of composition, and we use quantitative and qualitative indicators to provide baseline data for materials selection under MSR-relevant operating conditions [3,4].

2. Experimental

Wrought C276, SS316, and Alloy 600 coupons were exposed to the NaCl-$MgCl_2$ eutectic (58-42 mol%) under static (non-flow) conditions. Alumina crucibles sized to the hole pattern in the reactor top plate shown in Figure 1 were installed and then charged with the salt. Prior to mixing, $MgCl_2$ was step-dried below its melting point and NaCl was also dried, controlling residual moisture to ≤150 ppm ($MgCl_2$) and ≤50 ppm (NaCl), as verified by Karl Fischer titration. Coupons were suspended from the lowermost tier and the tier immediately above on the multi-level sample holder so that each specimen was fully immersed in the molten salt within its crucible; all other conditions were kept identical. Isothermal exposures were conducted at 650 ℃ and 550 ℃ for 500 h each. After cooling and rinsing to remove adherent salt, specimens were weighed to determine mass change; cross-sections were mounted and polished for SEM-EDS examination of corrosion morphology and elemental distributions, and XRD of surface layers was performed where required to identify corrosion products.

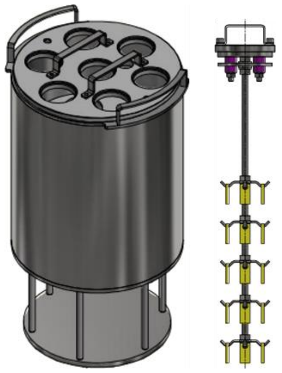

Figure 1. Schematic of reactor and sample holder for corrosion experiment

3. Results and Discussion

As seen in Figure 2, Alloy 600 and C276 commonly exhibited a thin, relatively continuous surface layer, a flat interface, and limited subsurface penetration. Although oxygen was observed near the interface, its co-distribution with Mg was not pronounced enough to form a continuous layer; thus, at 550 ℃, an MgO precipitated layer was not identified. Alloy 600 showed a narrow Feenriched band with slight Ni depletion at the interface, whereas C276 maintained Cr retention together with a flat interface. In contrast, SS316 developed grain-boundary-centered porous channels extending inward, accompanied by O enrichment and Fe depletion along those paths.

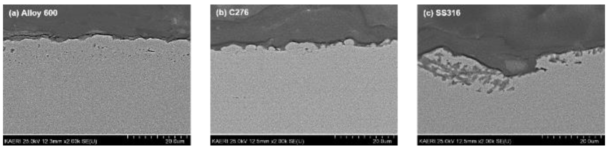

Figure 2. SEM images of each alloy at 550 ℃

As seen in Figure 3, damage became coarser overall, with clear alloy-dependent differences. Alloy 600 displayed the thinnest altered layer and a flat interface among the three alloys, with minimal subsurface penetration. C276 formed precipitated particles showing O-Mg co-distribution at the interface (interpreted as MgO), whereas SS316 did not exhibit an MgO precipitated layer. Chromium behavior can be summarized as follows: at 650 ℃, Cr depletion was not appreciable in Alloy 600, was local and of moderate extent in C276, and became thick and continuous in SS316.

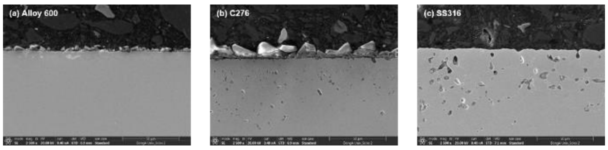

Figure 3. SEM images of each alloy at 650 ℃

To summarize, With increasing temperature from 550 to 650 °C, the damage mode clearly shifted from surface-limited attack to porous, grain-boundary-centered subsurface penetration, with SS316 showing the highest temperature sensitivity. At 650 ℃ alone, the morphological corrosion-resistance ranking was Alloy 600, C276, and SS316. And considering both temperatures together, the two Ni-rich alloys (Alloy 600 and C276) outperformed SS316. [5,6]

4. Conclusion

In the same NaCl-$MgCl_2$ environment, increasing the temperature from 550 to 650 ℃ shifted the damage mode toward grain-boundary-centered penetration. At 650 ℃, the morphological corrosion-resistance ranking was Alloy 600, C276 and SS316. An MgO precipitated layer was observed only on Alloy 600 and C276, and was absent on SS316. Chromium depletion followed SS316, C276 and Alloy 600, indicating that at high temperature Ni-rich alloys are relatively advantageous in terms of interfacial stability and compositional retention. However, this reflects an advantage from a corrosion perspective only; structural application also requires concurrent consideration of non-corrosion criteria such as high-temperature strength, creep resistance, elastic modulus, thermal expansion, cost, and manufacturability. Accordingly, for ~650 °C designs, this suggests that a mixed strategy—using an SS316 substrate with a Ni-rich overlay together with tight redox and moisture/oxygen control—may be a practical option.

ACKNOWLEDGMENTS

This work was supported by the Molten Salt Reactor Development Agency grant funded by the Korea government (the Ministry of Science and ICT) (Project Number: 1711198911)

REFERENCES

[1] O. Muransky, C. Yang, H. Zhu, et. al. “Molten salt corrosion of Ni-Mo-Cr candidate structural materials for Molten Salt Reactor (MSR) systems” Corrosion Science 159 (2019) 108087.

[2] B. Souza, A. Leong, Q. Yang, et. al. “Corrosion behavior of boronized nickel-based alloys in the molten chloride Salt” Corrosion Science 182 (2021) 109285

[3] G. McConohy, A. Kruizenga. “Molten nitrate salts at 600 and 680 ℃: Thermophysical property changes and corrosion of high-temperature nickel alloys” Solar Energy 103 (2014) 242-252

[4] D. F. Williams, L. M. Toth, K. T. Clarno. “Assessment of Candidate Molten Salt Coolants for the Advanced High-Temperature Reactor (AHTR)” ORNL/TM-2006/12

[5] L. Guo, Q. Liu, H. Yin, et. al. “Excellent corrosion resistance of 316 stainless steel in purified NaCl-$MgCl_2$ eutectic salt at high temperature” Corrosion Science 166 (2020) 108473

[6] S. Raiman, J. Kurley, D. Sulejmanovic, et. al. “Corrosion of 316H stainless steel in flowing FLiNaK salt” Journal of Nuclear Materials 561 (2022) 153551